다공확장벽을 이용한 미사일 동체에 대한 플룸간섭 현상의 제어

이영기* · 김희동**

Control of Plume Interference Effects on a Missile Body Using a Porous Extension

Young-Ki Lee* · Heuy-Dong Kim**

ABSTRACT

The physics of the plume-induced shock and separation particularly at a high plume to exit pressure ratio and supersonic speeds up to Mach 3.0 with and without a passive control method, porous extension, were studied using computational techniques. Mass-averaged Navier-Stokes equations with the RNG k-ε turbulence model were solved using a fully implicit finite volume scheme and a 4-stage Runge-Kutta method. The control methodology for plume-afterbody interactions is to use a perforated wall attached at either the nozzle exit or the edge of the missile base. The Effect of porous wall length on plume interference is also investigated. The computational results show the main effect of the porous extension on plume-afterbody interactions is to restrain the plume from strongly underexpanding during a change in flight conditions. With control, a change in porous extension length has no significant effect on plume interference.

초 록

플룸간섭 현상은 플룸에 의한 경계층 유동의 박리, 강한 전단층의 발생, 그리고 다수의 충격파들이 박리유동 및 전단층과 상호작용하게 되는 매우 복잡한 유동현상으로, 현재 미사일의 후미부에서 발생하는 플룸간섭 현상의 상세에 관해서는 잘 알려져 있지 않다. 본 연구에서는 초음속 미사일의 동체후미부에서 발생하는 플룸간섭 현상의 특징 및 동체기저부에 설치된 다공확장벽(porous extension)의 플룸간섭 현상에 대한 영향을 수치해석적으로 조사하였다. 그 결과, 다공확장벽이 플룸에 의한 충격파와 경계층 유동의 박리를 완화시켜 미사일 동체의 제어성능이 향상될 수 있음을 알았다.

Key Words: Supersonic Missile (초음속 미사일), Plume Interference (플룸간섭), Porous Extension (다공확장벽), Passive Control (피동제어), Shockwave (충격파)

† 2003년 10월13일 접수 ~ 2003년 12월 2일 심사완료
* 정회원, 안동대학교 기계공학부
** 종신회원, 안동대학교 기계공학부
연락저자, E-mail: kimhd@andong.ac.kr

1. Introduction

Supersonic speeds are the rule for most modern missiles, which require a very high thrust level within a limited cross sectional area. The aerodynamic designs in recent years, therefore, have focussed on understanding several problems associated with the plume expansion at high speeds and altitudes. These configurations generally have a highly underexpanded jet plume[1,2] downstream of the exhaust nozzle exit, leading to considerable interactions between the exhaust plume and freestream near the tail of missile bodies. The boundary layer separation[3,4] and pitching and yawing moments that result from the interactions can have significant effects on missile stability and control[5,6].

A detailed understanding of plume interference phenomena for an arbitrary missile configuration is indispensable to missile design. However, due to excessive assumptions to solve complex viscous-inviscid interactions and simple pressure measurements provided through most theoretical and experimental studies to date, the current knowledge base built in this research area is not adequate to provide an overall insight into the physics involved. CFD (Computational Fluid Dynamics) analyses, therefore, offer a way forward for the development of such a design. Very recently, some computational work[7,8] has been made mainly on base flow problems but, to the authors knowledge, no CFD study has been conducted for the control of plume interference phenomena.

In this research, a CFD investigation was conducted for missile models with a simple afterbody and with a porous extension to simulate highly underexpanded exhaust plumes at supersonic speeds. A fully implicit finite volume scheme was applied to mass-averaged Navier-Stokes equations with a two-equation turbulence model, RNG k-ε. The present numerical study may develop a basic understanding into the influence of the porous extension on the plume-induced shockwave and separation, leading to the effective and efficient control of flight bodies.

2. Numerical Simulations

Fig. 1 shows the schematic diagrams of missile models tested in this CFD analysis. The present computational model can be basically represented as an ogive forebody and straight afterbody without tail fins, identified as Simple. The 13-calibre missile body for the code validation had a 4-calibre tangent ogive nose and a cylindrical afterbody diameter of 63.5 mm. A convergent-divergent nozzle, having a design Mach number of 2.7, an exit diameter of D_e = 50.9 mm and a divergence half angle of 20°, was used to acquire supersonic plumes downstream of the nozzle exit. Porous extension models have a perforated wall with length l_p and porosity of 0.5, which is attached to either the afterbody edge (PD) or the nozzle exit (PDE). The afterbody models given here were tested in order to evaluate the effectiveness of the control of the flow features which may adversely affect overall missile performance.

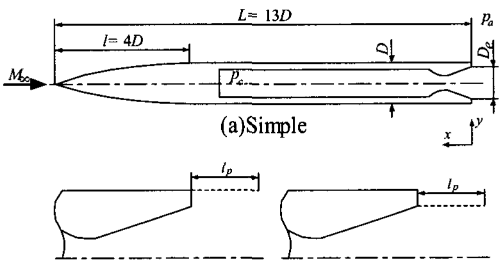

Fig. 1 Testing Model Configurations

Axisymmetric compressible Navier-Skokes computations were conducted via a commercial CFD code, Fluent 5, which has the ability to predict the flow fields involving strong shock interactions with shear layers and boundary layers so that is expected to provide high quality simulations for the flow fields around missile bodies with a highly underexpanded plume. The main parameter to characterize plume-freestream interactions is the freestream Mach number M_∞ up to 3.0 at a plume pressure ratio p_c/p_a of 170.9, which represents a highly underexpanded plume for the present missile models. Freestream pressure and temperature were assumed to be constant with values of 1 atm and 288.15 K respectively.

Basically, solutions were considered converged when the residuals for all equations drop by three orders of magnitude, typically 10^{-4} with the mass imbalance check for flow inlet and outlet boundaries.

3. Results and Discussion

The validation of the present computational code for M_∞ = 0.9 and 1.2 are given in Fig. 2. Static pressure distributions were measured from the end of the afterbody surface towards upstream with distance x. x and local static pressure along the missile surface were normalised by the model diameter D and atmospheric pressure p_a respectively. The results show reasonable agreement with the limited available pressure measurements[9]. At the lower Mach number of 0.9, the present code gave better predictions for the pressure rise before the plume expansion. However, with a stronger pressure rise at M_∞ = 1.2, the differences for the compression region become larger and these could be attributed to the inability of CFD code to accurately estimate a sharp pressure rise in this region. The fluctuations in the experimental pressure values upstream of the sharp pressure rise at M_∞ = 1.2 can result from support strut-plume interference and blockage effects in the wind tunnel tests.

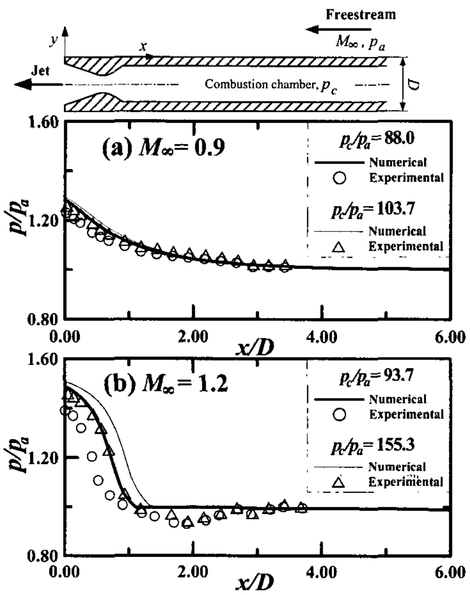

Fig. 2 Validation of the computational code with wind tunnel tests

Fig. 3(a) shows influences of the freestream Mach number on the static pressure distribution along the missile surface with a sharp corner for a fixed p_c/p_a of 170.9. As the Mach number increases from 1.2 to 3.0, the extent of shock-afterbody interaction is reduced and the shock moves downstream. It is considered that a stronger shear action at a relatively higher Mach number more strongly constrains the plume expansion and thus reduces the curvature of plume.

With an increase in the plume pressure ratio, there is an upstream movement of the plume -induced shock as observed in Fig. 3(b). It can be attributed to a stronger plume expansion downstream of the nozzle exit, resulting in increased expansion angle and dimensions of the plume. Then a larger turning angle of the flow approaching the plume boundary requires a stronger shock, leading to increased boundary layer separation near the trailing edge. It would be, therefore, helpful in design and the flight stability of a powered missile to control the plume-induced shock and separation on the afterbody surface without a significant modification to the geometry.

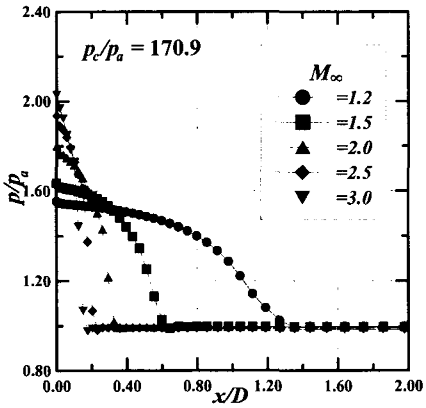

(a) Effect of the freestream Mach number

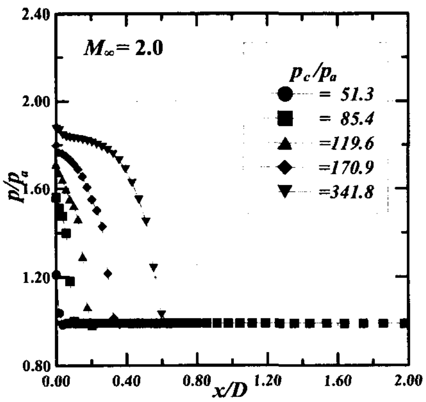

(b) Effect of the plume pressure ratio

Fig. 3 Wall static pressure distributions for Simple at supersonic speeds

At M_∞ = 2.0 and p_c/p_a = 170.9, Fig. 4 presents computed Schlieren images to describe the detailed flowfields in the control range for Simple and porous extension models. On the afterbody of Simple, a clear λ-shaped reflection of the shock system is generated by separation and reattachment of the boundary layer approaching the plume expansion. As a porous extension is attached to the nozzle exit (PDE), the shock moves to the tailing edge with a considerably reduced angle of plume expansion, flattening the curvature of the compression corner. On the other hand, as the device is attached to the afterbody edge (PD), no distinct downstream shock movement is observed though plume dimensions are smaller than those of Simple. It can be observed that PD produces intense flows emitted from the perforated wall, making the back flow in the separation region very strong and thus resulting in poor control performance.

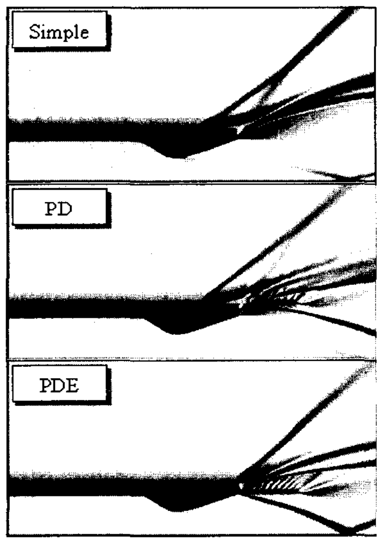

Fig. 4 Computed Schlieren images for Simple, PD and PDE (M_∞ = 2.0 and p_c/p_a = 170.9)

At M_∞ = 2.5 and p_c/p_a = 170.9, Fig. 5 shows the surface pressure distributions from the trailing edge towards upstream. When compared with Simple, PD gives no significant enhancement in shock movement and an increased pressure rise behind the shock while PDE results in a downstream location of the shock with reduced strength. The location of the porous extension, therefore, must be chosen carefully and the nozzle exit can be a good recommendation.

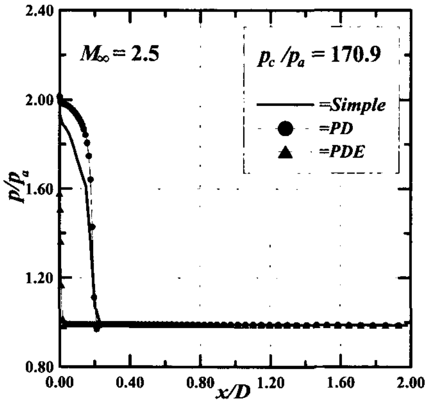

Fig. 5 Static pressure distributions along the afterbodies of Simple and porous extension models

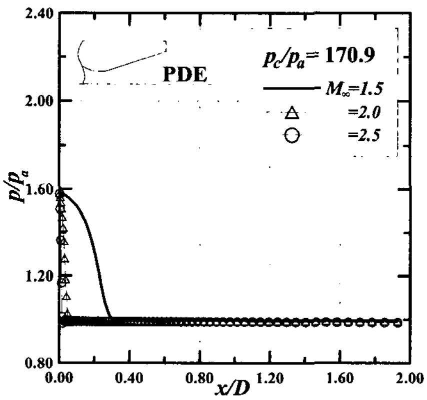

Fig. 6 Static pressure distributions along the afterbody of PDE

Pressure distributions in Fig. 6 explain the effects of the freestream Mach number on shock interactions in the cases a porous wall is attached at the missile base. The plume-induced shock largely moves downstream as the missile accelerates from Mach 1.5 to 2.0, but it is nearly fixed with a further increased Mach number. It is consider that the porous extension restrains the initial expansion of the plume near the nozzle exit, making the shock movement less severe. In the cases of fin-controlled missiles, the improved shock control in view of moving the shock away from the tail fin location or freezing the shock location may help the flight stability and control. In addition, reduced shock strength will lessen shock loading on the fin.

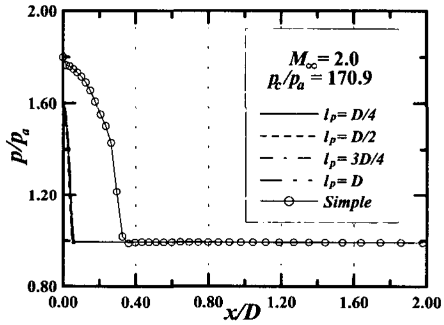

Fig. 7 Surface pressure distributions for PDE with various porous wall lengths

At M_∞ = 2.0 and p_c/p_a = 170.9, Fig. 7 shows the surface pressure distributions for several porous wall length l_p in the range of $D/4$ to D. Compared with Simple, a change in porous wall length has no significant effect on shock strength. In Fig. 8, it can be also observed that there is actually no variation in the shock location for different porous wall lengths except the case with l_p = $D/4$ and a low Mach number of 1.2, which shows a slight upstream location from other cases. Therefore, it is understood that the control of plume interference with a porous extension should be performed in consideration of the position of the device rather than its length.

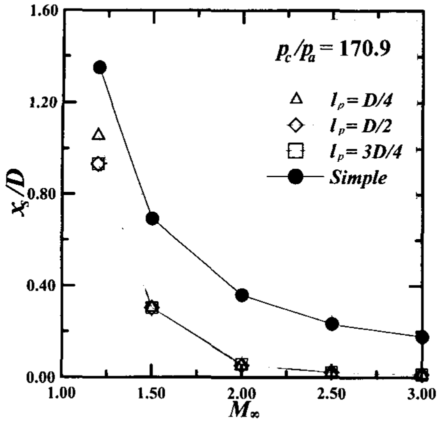

Fig. 8 Shock locations for several porous wall lengths

4. Conclusions

In the present work, missile models with a simple afterbody and with a porous extension at the missile base were simulated using axisymmetric Navier-Stokes computations. The compressible flowfield around the missile models at supersonic speeds was investigated at plume pressure ratios of 50 to 350 with an ogive forebody and a supersonic nozzle. The convergent-divergent nozzle with a design Mach number of 2.7 was selected to give moderately and highly underexpanded jets downstream of the nozzle.

The effect of a porous wall attached at the missile base on plume interference was mainly to restrain the plume from strongly underexpanding as the change in the flight condition. Control performance was strongly dependent on the device location but a change in porous extension length had no significant effect on the control. To effectively alleviate plume interference, therefore, this passive control method should be employed with an appropriate location of the device.

References

1. Albini, F. A., "Approximate Computation of Under-expanded Jet Structure," AIAA Journal, 1965, Vol.3, No.8, p.1538
2. Boynton, F. P., "Highly Under-expanded Jet Structure: Exact and Approximate Calculations," AIAA Journal, 1967, Vol.5, No.9, pp.1703-1704
3. Adamson, T. C. Jr. and Nicholls, J. A., "On the Structure of Jets from Highly Underexpanded Nozzles into Still Air," Journal of the Aeronautical Sciences, Jan. 1959, Vol.26, pp.16-24
4. Alpinieri, L. J. and Adams, R. H., "Flow Separation Due to Jet Pluming," AIAA Journal, Oct. 1966, Vol.4, No.10, pp.1865-1866
5. Fetterman, D. E. Jr., "Effects of Simulated Rocket-Jet Exhaust on Stability and Control of a Research-Type Airplane Configuration at a Mach Number of 6.86," NASA TM X-127, 1959
6. Yanowitch, S. and Hneuber, R. N., "Scout First Stage Flight Characteristics," NASA CR -111945, 1968
7. Matesanz, A., Velázquez, A., Perales, J. M. and Santiago-Prowald, J., "Numerical Simulation of Base-Flow/Plume Interaction," AIAA Paper 98-1597, 1998
8. Bannink, W. J., Houtman, E. M. and Bakker, P. G., "Base Flow/Underexpanded Exhaust Plume Interaction in a Supersonic External Flow," AIAA Paper 98-1598, 1998
9. Burt, J. R. Jr., "An Experimental Investigation of the Effect of Several Rocket Plume Simulators on the Pressure Distribution of a Body of Revolution at Free Stream Mach Number of 0.9 to 1.2," US Army Missile Command, Redstone Arsenal, Alabama, Technical Report RD-TR-70-23, Nov. 1970